Semileptonic decays of the B_c meson

M. A. Ivanov
Bogoliubov Laboratory of Theoretical Physics, Joint Institute for Nuclear Research, 141980 Dubna, Russia

J. G. Körner
Johannes Gutenberg-Universität, Institut für Physik, Staudinger Weg 7, D-55099, Mainz, Germany

P. Santorelli
Dipartimento di Scienze Fisiche, Università di Napoli ''Federico II,'' Italy
and INFN Sezione di Napoli, Via Cintia, I-80126 Napoli, Italy

(Received 17 July 2000; published 6 March 2001)

We study the semileptonic transitions $B_c \to \eta_c$, J/ψ, D, D^*, B, B^*, B_s, B_s^* in the framework of a relativistic constituent quark model. We use experimental data on leptonic J/ψ decay, lattice and QCD sum rule results on leptonic B_c decay, and experimental data on radiative η_c transitions to adjust the quark model parameters. We compute all form factors of the above semileptonic B_c transitions and give predictions for various semileptonic B_c decay modes including their τ modes when they are kinematically accessible. The implications of heavy quark symmetry for the semileptonic decays are discussed and are shown to be manifest in our explicit relativistic quark model calculation. A comparison of our results with the results of other calculations is performed.

DOI: 10.1103/PhysRevD.63.074010 PACS number(s): 13.20.He, 12.39.Ki

I. INTRODUCTION

Recently, the observation of the bottom-charm B_c meson at the Fermilab Tevatron has been reported by the Collider Detector at Fermilab (CDF) Collaboration [1]. The B_c mesons were found in the analysis of their semileptonic decays, $B_c^{\pm} \to J/\psi l^{\pm} X$. Values for the mass and the lifetime of the B_c meson were given as $M(B_c) = 6.40 \pm 0.39 \pm 0.13$ GeV and $\tau(B_c) = 0.46^{+0.18}_{-0.16}(\text{stat}) \pm 0.03(\text{syst})$ ps, respectively. The branching fraction for $B_c \to J/\psi\, l\, \nu$ relative to that for $B_c \to J/\psi K$ was found to be

$$\frac{\sigma(B_c)\times \text{Br}(B_c \to J/\psi l\, \nu)}{\sigma(B)\times \text{Br}(B_c \to J/\psi K)} = 0.132^{+0.041}_{-0.037}(\text{stat}) \pm 0.031(\text{syst})^{+0.032}_{-0.020}.$$

The study of the B_c meson is of great interest due to some of its outstanding features. It is the lowest bound state of two heavy quarks (charm and bottom) with open (explicit) flavor that can be compared with the charmonium ($c\bar{c}$ bound state) and the bottomium ($b\bar{b}$ bound state) which have hidden (implicit) flavor. The states with hidden flavor decay strongly and electromagnetically whereas the B_c meson decays weakly since it is below the $B\bar{D}$ threshold. Naively it might appear that the weak decays of the B_c meson are similar to those of the B and D mesons. However, the situation is quite different. The new spin-flavor symmetry arises for the systems containing one heavy quark when the mass of the heavy quark goes to infinity [2]. It gives some relations between the form factors of the physical processes. The deviations from heavy quark symmetry are large for the D meson and negligibly small for the B meson. On the contrary, in the case of the B_c meson a consistent heavy quark effective theory (for both constituent quarks) cannot include the heavy flavor symmetry [3]. However, the residual heavy quark spin symmetry can be used to reduce the number of independent semileptonic form factors at least near the zero recoil point [4].

In the naive spectator model, one would expect that $\Gamma(B_c) \approx \Gamma(B) + \Gamma(D)$ which gives $\tau(B_c) \approx 0.3$ ps, i.e. 1.5 times less than the central CDF value. The dominance of the $c \to s$ transition will have to be investigated in future analysis when more data become available. Thus a reliable evaluation of the long distance contributions is very important for studying the weak B_c decay properties.

The theoretical status of the B_c meson was reviewed in [5]. In this paper we focus on its exclusive leptonic and semileptonic decays which are sensitive to the description of long distance effects and are free of further assumptions, such as, for example, factorization of amplitudes in nonleptonic processes. Our results on the semileptonic transition form factors can of course be used for a calculation of the nonleptonic decays of the B_c meson using the factorization approach.

The exclusive semileptonic and nonleptonic (assuming factorization) decays of the B_c meson were calculated before in a potential model approach [6]. The binding energy and the wave function of the B_c meson were computed by using a flavor-independent potential with the parameters fixed by the $c\bar{c}$ and $b\bar{b}$ spectra and decays. The same processes were also studied in the framework of the Bethe-Salpeter equation in [7] and in the relativistic constituent quark model formulated on the light front in [8]. Three-point sum rules of QCD and nonrelativistic QCD (NRQCD) were analyzed in [9,10] to obtain the form factors of the semileptonic decays of $B_c^+ \to J/\psi(\eta_c) l^+ \nu$ and $B_c^+ \to B_s(B_s^*) l^+ \nu$.

As shown by the authors of [4], the form factors parametrizing the B_c semileptonic matrix elements can be related

to a smaller set of form factors if the decoupling of the spin of the heavy quarks in B_c and in the mesons produced in the semileptonic decays is exploited. The reduced form factors can be evaluated as overlap integral of the meson wave functions obtained, for example, using a relativistic potential model. This was performed in [11], where the B_c semileptonic form factors were computed and predictions for semileptonic and non-leptonic decay modes were given.

In this paper we employ the *relativistic constituent quark model* (RCQM) [12] for the description of B_c semileptonic meson decays. The RCQM is based on an effective Lagrangian describing the coupling of hadrons H to their constituent quarks, the coupling strength of which is determined by the compositeness condition $Z_H=0$ [13] where Z_H is the wave function renormalization constant of the hadron H. Here $Z_H^{1/2}$ is the matrix element between a physical particle state and the corresponding bare state. The compositeness condition $Z_H=0$ enables us to represent a bound state by introducing a quasiparticle interacting with its constituents so that the renormalization factor is equal to zero. This does not mean that we can solve the QCD bound state equations but we are able to show that the condition $Z_H=0$ provides an effective and self-consistent way to describe the coupling of the particle to its constituents. One starts with an effective Lagrangian written down in terms of quark and hadron variables. Then, by using Feynman rules, the S-matrix elements describing hadronic interactions are given in terms of a set of quark diagrams. In particular, the compositeness condition enables one to avoid a double counting of hadronic degrees of freedom. This approach is self-consistent and all calculations of physical observables are straightforward. There is a small set of model parameters: the values of the constituent quark masses and the scale parameters that define the size of the distribution of the constituent quarks inside a given hadron. This distribution can be related to the relevant Bethe-Salpeter amplitudes.

The shapes of the vertex functions and the quark propagators can in principle be found from an analysis of the Bethe-Salpeter and Dyson-Schwinger equations, respectively, as done e.g. in [15]. The Dyson-Schwinger equation (DSE) has been employed to entail a unified and uniformly accurate description of light- and heavy-meson observables [16]. In this paper we, however, choose a more phenomenological approach where the vertex function is modeled by a Gaussian form, the size parameter of which is determined by a fit to the leptonic and radiative decays of the lowest lying charm and bottom mesons. For the quark propagators we use the local representation.

The leptonic and semileptonic decays of the lower-lying pseudoscalar mesons (π, K, D, D_s, B, B_s) have been described in Ref. [17] in which a Gaussian form was used for the vertex function and free propagators were adopted for the constituent quarks. The adjustable parameters, the widths of Bethe-Salpeter amplitudes in momentum space and the constituent quark masses were determined from a least squares fit to available experimental data and some lattice determinations. We found that our results are in good agreement with experimental data and other approaches. It was also shown that the scaling relations resulting from the spin-flavor symmetries are reproduced by the model in the heavy quark limit.

Using this approach we have elaborated the so-called *relativistic three-quark model* (RTQM) to study the properties of heavy baryons containing a single heavy quark (bottom or charm). For the heavy quarks we used propagators appropriate for the heavy quark limit. Physical observables for the semileptonic and nonleptonic decays as well as for the one-pion and one-photon transitions have been successfully described in this approach [18]. Recently, the RTQM was extended to include the effects of finite quark masses [19]. We mention that the authors of [20] have developed a relativistic quark model approach to the description of meson transitions which has similarities to our approach. They also use an effective heavy meson Lagrangian to describe the couplings of mesons to quarks. They use, however, point-like meson-quark interactions. Loop momenta are explicitly cut off at around 1 GeV in the approach [20]. In our approach we use momentum dependent meson-quark interactions, which provides for an effective cutoff of the loop integration. We would also like to mention a recent investigation [21] where the same quark-meson Lagrangian employed in [12] was used. The authors of [21] employed dipole vertex to describe various leptonic and semileptonic decays of both the heavy-light mesons and the B_c meson.

In this paper we follow the strategy adopted in Refs. [16,17]. The basic assumption on the choice of the vertex function in the hadronic matrix elements is made after transition to momentum space. We employ the impulse approximation in calculating these matrix elements which has been used widely in phenomenological DSE studies (see, e.g., Ref. [16]). In the impulse approximation one assumes that the vertex functions depend only on the loop momentum flowing through the vertex. We present a general method which greatly facilitates the numerical evaluations that occur in the Feynman-type calculations involving quark loops (see also [12,17]).

The basic emphasis of this work is to study leptonic and semileptonic decays of the B_c meson. We use Gaussian vertex functions with size parameters for heavy-light mesons as in Ref. [17]. In this paper we limit our attention to the basic semileptonic decay modes of the B_c meson. A new feature of our calculation is that we also discuss semileptonic decays involving the τ lepton. We discuss in some detail how our quark loop calculations reproduce the heavy quark limit relations between form factors at zero recoil. Explicit expressions for the reduced set of form factors in this limit are given.

II. MODEL

We employ an approach [12] based on the effective interaction Lagrangian which describes the coupling between hadrons and their constituent quarks. For example, the coupling of the meson H into its constituents q_1 and q_2 is given by the Lagrangian

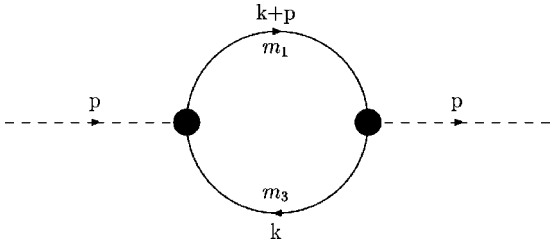

FIG. 1. One-loop self-energy type diagram needed for the evaluation of the compositeness condition.

$$\mathcal{L}_{\rm int}(x)=g_H H(x)\int dx_1\int dx_2\Phi_H(x,x_1,x_2)\times\bar{q}(x_1)\Gamma_H\lambda_H q(x_2). \quad (2.1)$$

Here, λ_H and Γ_H are Gell-Mann and Dirac matrices, respectively, which entail the flavor and spin quantum numbers of the meson H. The function Φ_H is related to the scalar part of Bethe-Salpeter amplitude and characterizes the finite size of the meson. Φ_H is invariant under the translation $\Phi_H(x+a,x_1+a,x_2+a)=\Phi_H(x,x_1,x_2)$ which is necessary for the Lorence invariance of the Lagrangian (2.1). For instance, the separable form

$$\Phi_H(x,x_1,x_2)=\delta\left(x-\frac{x_1+x_2}{2}\right)f((x_1-x_2)^2) \quad (2.2)$$

has been used in [12] for pions with $f(x^2)$ being a Gaussian. The straightforward generalization of the vertex function (2.2) to the case of an arbitrary pair of quarks with different masses is given by

$$\Phi_H(x,x_1,x_2)=\delta\left(x-\frac{m_1x_1+m_2x_2}{m_1+m_2}\right)f((x_1-x_2)^2). \quad (2.3)$$

The authors of [21] used a dipole form for the Fourier transform of the function $f(x^2)$. Here we follow the slightly different strategy as proposed in Refs. [16,17]. The choice of the vertex function in the hadronic matrix elements is specified after transition to momentum space. We employ the impulse approximation in calculating the one-loop transition amplitudes. In the impulse approximation one assumes that the vertex functions depend only on the loop momentum flowing through the vertex. The impulse approximation has been used widely in phenomenological DSE studies (see, e.g., Ref. [16]). The final results of calculating a quark loop diagram depend on the choice of loop momentum flow. In the heavy quark transitions discussed in this paper the loop momentum flow is, however, fixed if one wants to reproduce the heavy quark symmetry results.

To demonstrate our assumption, we consider the meson mass function defined by the diagram in Fig. 1. We have

$$\Pi_H(x-y)=\int dx_1\int dx_2\Phi_H(x,x_1,x_2)\times\int dy_1\int dy_2\Phi_H(y,y_1,y_2)\times{\rm tr}\{S(y_1-x_1)\Gamma_H S(x_2-y_2)\Gamma_H\}. \quad (2.4)$$

Then we calculate the Fourier transform of the meson mass function (2.4):

$$\begin{aligned}\tilde{\Pi}_H(p)&=\int e^{-ipx}\Pi_H(x)\\&=\int\frac{dq}{(2\pi)^4}\int\frac{dk_1}{(2\pi)^4}\int\frac{dk_2}{(2\pi)^4}\tilde{\Phi}_H\times(-p,k_1,-k_2)\tilde{\Phi}_H(q,-k_1,k_2)\times{\rm tr}\{S(\not k_1)\Gamma_H S(\not k_2)\Gamma_H\}. \quad (2.5)\end{aligned}$$

The Fourier transform of the function $\Phi(x_1,\ldots,x_n)$ which is invariant under the translation $x_i\to x_i+a$ can be written as

$$\begin{aligned}\tilde{\Phi}(q_1,\ldots,q_n)&=\int dx_1\cdots\int dx_n\times\exp\left(i\sum_{i=1}^n x_iq_i\right)\Phi(x_1,\ldots,x_n)\\&\times(2\pi)^4\delta\left(\sum_{i=1}^n q_i\right)n^4\int dx_1\cdots\int dx_n\times\delta\left(\sum_{i=1}^n x_i\right)\exp\left(i\sum_{i=1}^n x_iq_i\right)\Phi(x_1,\ldots,x_n)\\&\equiv(2\pi)^4\delta\left(\sum_{i=1}^n q_i\right)\phi(q_1,\ldots,q_{n-1}). \quad (2.6)\end{aligned}$$

Using this property one finds

$$\tilde{\Pi}_H(p)=\int\frac{dk}{(2\pi)^4}\phi_H^2(k,p){\rm tr}\{S(\not k+\not p)\Gamma_H S(\not k)\Gamma_H\}. \quad (2.7)$$

Here, we assume that the vertex function ϕ_H depends only on the loop momentum k. Besides, we assume that ϕ_H is analytical function which decreases sufficiently fast in the Euclidean momentum space to render all loop diagrams UV finite.

The coupling constants g_H are determined by the so-called *compositeness condition* proposed in [13] and extensively used in [14]. The compositeness condition means that the renormalization constant of the meson field is equal to zero,

$$Z_H=1-\frac{3g_H^2}{4\pi^2}\tilde{\Pi}'_H(m_H^2)=0, \quad (2.8)$$

where $\tilde{\Pi}'_H$ is the derivative of the meson mass function defined by the diagram in Fig. 1:

$$\Pi_P(p^2)=\int \frac{d^4k}{4\pi^2 i}\phi_P^2(-k^2)\mathrm{tr}[\gamma^5 S_3(\not k+m_3)\gamma^5 S_1(\not k+\not p+m_1)], \tag{2.9}$$

$$\Pi_V(p^2)=\frac{1}{3}\left[g^{\mu\nu}-\frac{p^\mu p^\nu}{p^2}\right]\int \frac{d^4k}{4\pi^2 i}\phi_V^2(-k^2) \times \mathrm{tr}[\gamma^\mu S_3(\not k+m_3)\gamma^\nu S_1(\not k+\not p+m_1)]. \tag{2.10}$$

For simplicity, we extract the factor $1/4\pi^2$ from the definition of the meson mass operator. We use the local quark propagators

$$S_i(\not k)=\frac{1}{m_i-\not k}, \tag{2.11}$$

where m_i is the constituent quark mass. As discussed in [12], we assume that $m_H<m_{q_1}+m_{q_2}$ in order to avoid the appearance of imaginary parts in the physical amplitudes. This is a reliable approximation for the heavy pseudoscalar mesons. The above condition is not always met for heavy vector mesons. As discussed in Sec. VI we shall therefore employ equal masses for the heavy pseudoscalar and vector mesons in our matrix element calculations but use physical masses for the phase space.

III. METHOD FOR THE EVALUATION OF ONE-LOOP DIAGRAMS WITH ARBITRARY VERTEX FUNCTIONS

For the present purposes one has to evaluate one-loop integrals of two- and three-point functions involving tensor integrands and product of vertex functions. In this section we describe a general method to efficiently enact these calculations for the general case of *n*-point one-loop functions. We note two simplifying features of our integration technique. The arising tensor integrals are reduced to simple invariant integrations. The sequence of integrations is arranged such that the product of vertex functions is kept to the very end and allowing for a full flexibility in the choice of vertex functions.

We consider a rank *s* tensor integral in the Minkowski space as it appears in a general one fermion-loop calculation of an *n*-point function (see the diagram in Fig. 2). One has

$$I^{\mu_1,\ldots,\mu_s}_{[n,s]}=\int \frac{d^4k}{i\pi^2}\mathcal{F}(-k^2)\frac{k^{\mu_1}\cdots k^{\mu_s}}{\prod_{i=1}^{n}[m_i^2-(k+l_i)^2]}. \tag{3.1}$$

The outer momenta p_j $(j=1,\ldots,n)$ are all taken to be incoming. The momenta of the inner lines are given by $k+l_i$ with $l_i=\Sigma_{j=1}^{i}p_j$ such that $l_n=0$. The maximum degree of the momentum tensor in the numerator arising from the *n* fermion propagators is $s_{\max}=n$. We employ the impulse approximation dropping the dependence on the external momenta inside the vertex functions and denote the product of all vertex functions by $\mathcal{F}(-k^2)$.

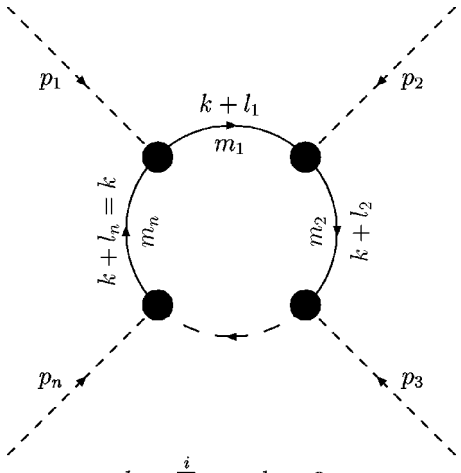

FIG. 2. One-loop diagram with *n* legs and arbitrary vertex functions.

Using the α parametrization of Feynman one finds

$$I^{\mu_1,\ldots,\mu_s}_{[n,s]}=\Gamma(n)\int d^n\alpha\,\delta\left(1-\sum_{i=1}^{n}\alpha_i\right) \times\int \frac{d^4k}{i\pi^2}\mathcal{F}(-k^2)\frac{k^{\mu_1}\cdots k^{\mu_s}}{[D_n(\alpha)-(k+P)^2]^n}, \tag{3.2}$$

where $P=\Sigma_{i=1}^{n}\alpha_i l_i$, and $D_n(\alpha)=\Sigma_{i,j}\alpha_i\alpha_j d_{ij}$ with $d_{i,j}=(1/2)\,[m_i^2+m_j^2-(l_i-l_j)^2]$.

Next we use the Cauchy integral representation for the function $\mathcal{F}(-k^2)$ leading to

$$I^{\mu_1,\ldots,\mu_s}_{[n,s]}=\Gamma(n)\int d^n\alpha\,\delta\left(1-\sum_{i=1}^{n}\alpha_i\right) \times\int \frac{d^4k}{i\pi^2}\oint\frac{d\zeta\mathcal{F}(-\zeta)}{2\pi i} \times\frac{k^{\mu_1}\cdots k^{\mu_s}}{[\zeta-k^2][D_n(\alpha)-(k+P)^2]^n}.$$

The new denominator factor is then included again via Feynman parametrization, giving

$$I^{\mu_1,\ldots,\mu_s}_{[n,s]}=\Gamma(n+1)\int_0^1 d\beta\beta^{n-1}\int d^n\alpha\,\delta\left(1-\sum_{i=1}^{n}\alpha_i\right)\int\frac{d^4k}{i\pi^2}\oint\frac{d\zeta\mathcal{F}(-\zeta)}{2\pi i}\times\frac{k^{\mu_1}\cdots k^{\mu_s}}{[(1-\beta)\zeta-(k+\beta P)^2+\beta D_n(\alpha)-\beta(1-\beta)P^2]^{n+1}}.$$

One then factors out the $(1-\beta)$ in the denominator and shifts the integration variable k to $k'=(k+\beta P)/\sqrt{1-\beta}$ to obtain

$$I^{\mu_1,\ldots,\mu_s}_{[n,s]}=\Gamma(n+1)\int_0^1 d\beta\left(\frac{\beta}{1-\beta}\right)^{n-1}\int d^n\alpha\times\delta\left(1-\sum_{i=1}^{n}\alpha_i\right)\int\frac{d^4k}{i\pi^2}\oint\frac{d\zeta\mathcal{F}(-\zeta)}{2\pi i}\times\frac{(\sqrt{1-\beta}k-\beta P)^{\mu_1}\cdots(\sqrt{1-\beta}k-\beta P)^{\mu_s}}{[\zeta-k^2+z]^{n+1}}.$$

The contour integral can be done again by Cauchy's theorem. On substitution of $\beta=t/(1+t)$ one then has

$$I^{\mu_1,\ldots,\mu_s}_{[n,s]}=(-)^n\int_0^\infty dt\frac{t^{n-1}}{(1+t)^2}\int d^n\alpha\times\delta\left(1-\sum_{i=1}^{n}\alpha_i\right)\int\frac{d^4k}{i\pi^2}\mathcal{F}^{(n)}(-k^2+z)K^{\mu_1}\cdots K^{\mu_s},$$

where $\mathcal{F}^{(n)}$ denotes the nth derivative of the function $\mathcal{F}$ and where

$$K^\mu=\frac{1}{\sqrt{1+t}}k^\mu-\frac{t}{1+t}P^\mu,\quad z=t\,D_n(\alpha)-\frac{t}{1+t}P^2.$$

The momentum integration of the tensor integral can be trivially done by invariant integration. Finally we go to the Euclidean space by rotating $k_0\to ik_4$ which gives $k^2\to-k_E^2\equiv u$; then one encounters the scalar integrals

$$I_{[n,m]}=(-)^n\int_0^\infty dt\frac{t^{n-1}}{(1+t)^{2+m}}\int d^n\alpha\times\delta\left(1-\sum_{i=1}^{n}\alpha_i\right)\int_0^\infty du u^{m+1}\mathcal{F}^{(n)}(u+z).\quad(3.3)$$

The u integration can be performed by partial integration and one finally obtains

$$I_{[n,m]}=(-)^{n+m}\Gamma(m+2)\int_0^\infty dt\frac{t^{n-1}}{(1+t)^{2+m}}\int d^n\alpha\times\delta\left(1-\sum_{i=1}^{n}\alpha_i\right)\mathcal{F}^{(n-m-2)}(z).\quad(3.4)$$

Since $m_{\max}=[n/2]$, Eq. (3.4) holds true for all n and m except for the case $n=2$ and $m=1$. In this case we have

$$I_{[2,1]}=2\int_0^\infty dt\frac{t}{(1+t)^3}\int d^2\alpha\,\delta\left(1-\sum_{i=1}^{2}\alpha_i\right)\int_z^\infty du\mathcal{F}(u)=\int_0^\infty dt\left(\frac{t}{1+t}\right)^2\int d^2\alpha\,\delta\left(1-\sum_{i=1}^{2}\alpha_i\right)z_t'\mathcal{F}(z),\quad(3.5)$$

where $z_t'=dz(t)/dt$.

One has to remark that the integration over the α parameters in Eq. (3.4) can be done analytically up to a remaining one-fold integral. However, the ease with which the numerical α integrations can be done does not warrant the effort of further analytical integrations. Using the integration techniques described in this section all necessary numerical integrations encountered in this investigation can be performed within minutes using a fast modern PC.

IV. HADRONIC MATRIX ELEMENTS

A. Quark-meson coupling constants

As already discussed in Sec. II, the quark-meson coupling constants are determined by the compositeness condition, Eq. (2.8). The derivatives of the meson-mass functions can be written as

$$\frac{d}{dp^2}\Pi_P(p^2)=\frac{1}{2p^2}p^\alpha\frac{d}{dp^\alpha}\int\frac{d^4k}{4\pi^2 i}\phi_P^2(-k^2)\times\mathrm{tr}[\gamma^5 S_3(\not k)\gamma^5 S_1(\not k+\not p)]=\frac{1}{2p^2}\int\frac{d^4k}{4\pi^2 i}\phi_P^2(-k^2)\times\mathrm{tr}[\gamma^5 S_3(\not k)\gamma^5 S_1(\not k+\not p)\not p\, S_1(\not k+\not p)],\quad(4.1)$$

$$\frac{d}{dp^2}\Pi_V(p^2)=\frac{1}{3}\frac{1}{2p^2}p^\alpha\frac{d}{dp^\alpha}\left[g^{\mu\nu}-\frac{p^\mu p^\nu}{p^2}\right]\times\int\frac{d^4k}{4\pi^2 i}\phi_V^2(-k^2)\times\mathrm{tr}[\gamma^\mu S_3(\not k)\gamma^\nu S_1(\not k+\not p)]$$

$$= \frac{1}{3}\left[g^{\mu\nu} - \frac{p^\mu p^\nu}{p^2}\right]\frac{1}{2p^2}\int \frac{d^4k}{4\pi^2 i}\,\phi_V^2(-k^2)$$
$$\times \mathrm{tr}[\,\gamma^\mu S_3(k)\,\gamma^\nu S_1(k+p)\not{p}\,S_1(k+p)]. \tag{4.2}$$

The evaluation of the integrals is done by using the method outlined in Sec. III. The compositeness condition reads

$$\frac{3g_H^2}{4\pi^2}N_H = 1, \quad \text{where} \quad N_H = \frac{d}{dp^2}\Pi_H(p^2)\bigg|_{p^2=m_H^2} \tag{4.3}$$

$$N_H = \frac{1}{2}\int_0^\infty dt\left(\frac{t}{1+t}\right)^2\int_0^1 d\alpha\,\alpha\{\cdots\}_H$$

$$\{\cdots\}_P = \mathcal{F}_P(z)\frac{1}{1+t}\left[4-3\frac{\alpha t}{1+t}\right] - \mathcal{F}_P'(z)$$
$$\times\left\{2m_1m_3 + \frac{\alpha t}{1+t}[m_1^2 - 2m_1m_3 + p^2]\right.$$
$$\left. - p^2\left(\frac{\alpha t}{1+t}\right)^2\left(2-\frac{\alpha t}{1+t}\right)\right\},$$

$$\{\cdots\}_V = \mathcal{F}_V(z)\frac{1}{1+t}\left[2-\frac{\alpha t}{1+t}\right] - \mathcal{F}_V'(z)$$
$$\times\left\{2m_1m_3 + \frac{\alpha t}{1+t}[m_1^2 - 2m_1m_3 + p^2]\right.$$
$$\left. - p^2\left(\frac{\alpha t}{1+t}\right)^2\left(2-\frac{\alpha t}{1+t}\right)\right\}.$$

Here, m_1 stands for the heavy quark (b or c) and m_2 for the light quarks (u, d, s) in the case of heavy-light systems, and for c in the case of double-heavy systems. The function $\mathcal{F}_H(z)$ is the product of two vertex functions $\mathcal{F}_H(z) = \phi_H^2(z)$ with

$$z = t[\,\alpha m_1^2 + (1-\alpha)m_3^2 - \alpha(1-\alpha)p^2] - \frac{\alpha^2 t}{1+t}p^2.$$

B. Leptonic and radiative decays

The matrix elements of the leptonic and radiative decays are defined by the diagrams in Figs. 3–6 and given by

$$iM_P^\mu(p) = \frac{3g_P}{4\pi^2}\int \frac{d^4k}{4\pi^2 i}\,\phi_P(-k^2)$$
$$\times \mathrm{tr}[\,\gamma^5 S_3(k) O^\mu S_1(k+p)]$$
$$= f_P p^\mu, \tag{4.4}$$

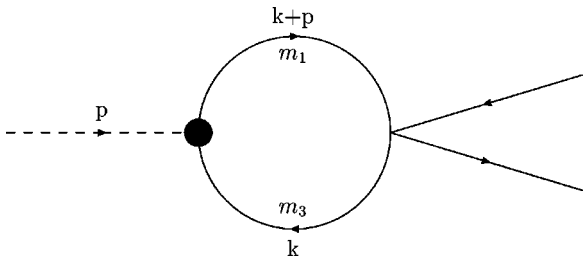

FIG. 3. Quark model diagram for leptonic meson decays.

$$M_V^\mu(p) = -C_V\cdot\frac{3g_V}{4\pi^2}\int\frac{d^4k}{4\pi^2 i}\,\phi_V(-k^2)$$
$$\times \mathrm{tr}[\,\not{\epsilon}^* S_q(k)\,\gamma^\mu S_q(k+p)]$$
$$= -m_V C_V f_V \epsilon^{*\mu}, \tag{4.5}$$

$$iM_{P\gamma\gamma}(q_1,q_2) = C_{P\gamma\gamma}\frac{3g_P}{4\pi^2}\int\frac{d^4k}{4\pi^2 i}\,\phi_P(-k^2)$$
$$\times \mathrm{tr}[\,\gamma^5 S_q(k-\not{q}_2)\not{\epsilon}_2^* S_q(k)\not{\epsilon}_1^* S_q(k+\not{q}_1)],$$
$$= ig_{P\gamma\gamma}\varepsilon^{\mu\nu\alpha\beta}\epsilon_1^{*\mu}\epsilon_2^{*\nu}q_1^\alpha q_2^\beta, \tag{4.6}$$

$$iM_{VP\gamma}(p,p') = C_{VP\gamma}\frac{3g_V g_P}{4\pi^2}\int\frac{d^4k}{4\pi^2 i}\mathcal{F}_{PV}(-k^2)$$
$$\times \mathrm{tr}[\,\gamma^5 S_q(k+\not{p})\not{\epsilon}^* S_q(k)\not{\epsilon}_\gamma^* S_q(k+\not{q})]$$
$$= ig_{VP\gamma}\varepsilon^{\mu\nu\alpha\beta}\epsilon_\gamma^{*\mu}\epsilon^{*\nu}p^\alpha q^\beta. \tag{4.7}$$

For ease of presentation, the expression for the $V\to P\gamma$ decay is given for neutral-flavored mesons. Using the integration techniques described in Sec. III one then arrives at the following analytical representation of the various one-loop matrix elements:

$$f_P = \frac{3g_P}{4\pi^2}\int_0^\infty dt\frac{t}{(1+t)^2}\int_0^1 d\alpha\,\phi_P(z_P)$$
$$\times\left[m_3 + (m_1-m_3)\frac{\alpha t}{1+t}\right],$$

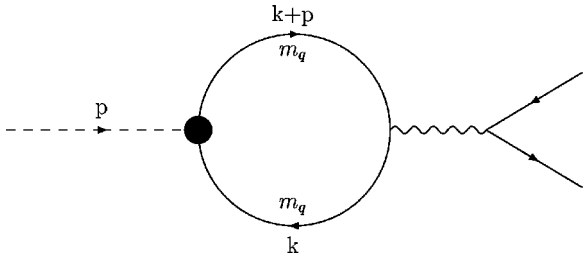

FIG. 4. Quark model diagram for vector meson radiative decays.

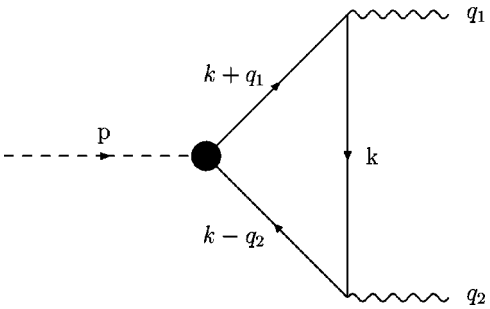

FIG. 5. Quark model diagram for the decays of a neutral meson.

$$z_P = t[\alpha m_1^2 + (1-\alpha)m_3^2 - \alpha(1-\alpha)p^2] - \frac{t\alpha^2}{1+t}p^2, \tag{4.8}$$

$$f_V = \frac{1}{m_V}\frac{3g_V}{4\pi^2}\int_0^\infty dt \frac{t}{(1+t)^2}\int_0^1 d\alpha \phi_V(z_V) \times\left[m_q^2 + \frac{1}{2}tz_t' + \frac{\alpha t}{1+t}\left(1-\frac{\alpha t}{1+t}\right)p^2\right],$$

$$z_V = t[m_q^2 - \alpha(1-\alpha)p^2] - \frac{t\alpha^2}{1+t}p^2,$$

$$\Gamma(V\to e^+e^-) = \frac{4\pi}{3}\frac{\alpha^2}{m_V}f_V^2 C_V^2, \quad C_V = e_q^2 (V=\phi, J/\psi, \Upsilon), \tag{4.9}$$

$$g_{P\gamma\gamma} = C_{P\gamma\gamma} m_q \frac{3g_P}{4\pi^2}\int_0^\infty dt\left(\frac{t}{1+t}\right)^2 \times\int d^3\alpha\,\delta\left(1-\sum_{i=1}^3 \alpha_i\right)[-\phi_P'(z_0)],$$

$$z_0 = t(m_q^2 - \alpha_1\alpha_2 p^2) - \frac{t}{1+t}\alpha_1\alpha_2 p^2,$$

$$\Gamma(P\to\gamma\gamma) = \frac{\pi}{4}\alpha^2 m_P^3 g_{P\gamma\gamma}^2, \quad C_{\eta_c\gamma\gamma} = 2e_c^2, \tag{4.10}$$

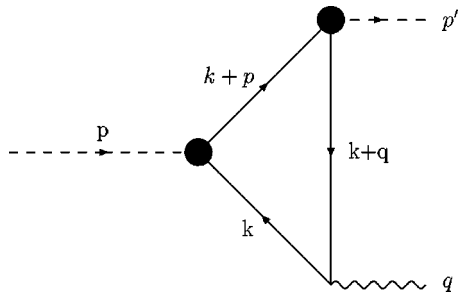

FIG. 6. Quark model diagram for the radiative decay of a vector meson into a pseudoscalar one.

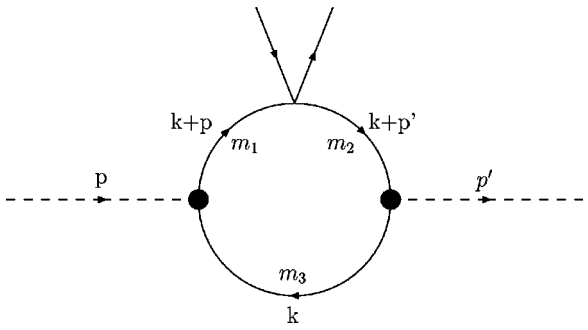

FIG. 7. Quark model diagram for the semileptonic B_c decays involving $b\to c,u$ transitions. The lower leg in the loop is the c quark.

$$g_{VP\gamma} = C_{VP\gamma} m_q \frac{3g_V g_P}{4\pi^2}\int_0^\infty dt\left(\frac{t}{1+t}\right)^2 \times\int d^3\alpha\,\delta\left(1-\sum_{i=1}^3 \alpha_i\right)[-\mathcal{F}_{VP}'(z_{VP})],$$

$$z_{VP} = t(m_q^2 - \alpha_1\alpha_3 m_V^2 - \alpha_1\alpha_2 m_P^2) - \frac{t}{1+t}[\alpha_1(\alpha_1+\alpha_2)m_V^2 - \alpha_1\alpha_2 m_P^2],$$

$$\Gamma(V\to P\gamma) = \frac{\alpha}{24}m_V^3\left(1-\frac{m_P^2}{m_V^2}\right)^3 g_{VP\gamma}^2 \quad C_{J/\psi\eta_c\gamma} = 2e_c. \tag{4.11}$$

The electric quark charges e_q are given in units of e.

C. Semileptonic form factors

The semileptonic decays of the B_c meson can be induced by either a beauty quark or a charm quark transition. In the relativistic quark model, the hadronic matrix element corresponding to b decay is defined by the diagram in Fig. 7 and is given by

$$M_b^\mu(P(p)\to H(p')) = \frac{3g_P g_H}{4\pi^2}\int\frac{d^4k}{4\pi^2 i}\mathcal{F}_{PH}(-k^2) \times \mathrm{tr}[\gamma^5 S_3(\not k)\Gamma_H S_2(\not k + \not p')O^\mu S_1(\not k + \not p)], \tag{4.12}$$

where $\mathcal{F}_{PH} = \phi_P\cdot\phi_H$, $\Gamma_P = \gamma^5$, and $\Gamma_V = -i\not\epsilon^*$ with $\epsilon^*\cdot p' = 0$. For the b-decay case one has the Cabibbo-Kobayaski-Maskawa- (CKM)-enhanced decays

$$b\to c: \quad B_c^+ \to (\eta_c, J/\psi) l^+\nu, \quad m_1 = m_b, \; m_2 = m_3 = m_c,$$

and the CKM-suppressed decays

$$b\to u: \quad B_c^+ \to (D^0, D^{*0}) l^+\nu, \quad m_1 = m_b,$$

$$m_2 = m_u, \; m_3 = m_c.$$

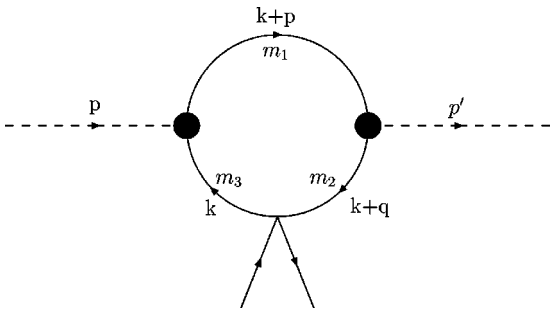

FIG. 8. Quark model diagram for the semileptonic B_c decays involving $c\to s,d$ transitions. The upper leg in the loop is the b quark.

The c-decay option of the B_c meson is represented by the Feynman diagram in Fig. 8 which gives

$$M_c^\mu(P(p)\to H(p')) = \frac{3g_P g_H}{4\pi^2}\int \frac{d^4k}{4\pi^2 i}\mathcal{F}_{PH}(-k^2) \times \mathrm{tr}[\gamma^5 S_3(\not k) O^\mu S_2(\not k+\not q)\Gamma_H S_1(\not k+\not p)]. \tag{4.13}$$

Again one has the CKM-enhanced decays

$$c\to s:\quad B_c^+\to(\bar B_s^0,\bar B_s^{*0})l^+\nu,\quad m_1=m_b,\quad m_2=m_s,\quad m_3=m_c,$$

and the CKM-suppressed decays

$$c\to d:\quad B_c^+\to(\bar B^0,\bar B^{*0})l^+\nu,\quad m_1=m_b,\quad m_2=m_d,\quad m_3=m_c.$$

It is convenient to present the results of the matrix element evaluations in terms of invariant form factors. A standard decomposition of the transition matrix elements into invariant form factors is given by

$$M^\mu(P(p)\to P'(p')) = f_+(q^2)(p+p')^\mu + f_-(q^2)(p-p')^\mu \tag{4.14}$$

and

$$iM^\mu(P(p)\to V(p')) = -g^{\mu\nu}\epsilon^{*\nu}(m_P+m_V)A_1(q^2)+(p+p')^\mu p\cdot\epsilon^* \times\frac{A_2(q^2)}{m_P+m_V}+(p-p')^\mu p\cdot\epsilon^* \times\frac{A_3(q^2)}{m_P+m_V}-i\varepsilon^{\mu\nu\alpha\beta}\epsilon^{*\nu}p^\alpha p'^\beta\frac{2V(q^2)}{m_P+m_V}. \tag{4.15}$$

The various invariant form factors can be extracted from the one-loop expressions (4.12) and (4.13) by using the techniques described in Sec. III. One finds that the form factor integrands factorize into a common piece times a piece specific to the different form factors. One can thus write

$$F(q^2)=\frac{3}{4\pi^2}g_P g_H\frac{1}{2}\int_0^\infty dt\left(\frac{t}{1+t}\right)^2\int d^3\alpha\,\delta\left(1-\sum_{i=1}^3\alpha_i\right)\times\{\cdots\}_F \tag{4.16}$$

where $F=f_\pm,A_i,V$. For the $0^-\to0^-$ $b\to c,u$ form factors f_+ one has

$$\{\cdots\}^b_{f_+}=\mathcal{F}_{PP}(z_b)\frac{1}{1+t}\left[4-3(\alpha_1+\alpha_2)\frac{t}{1+t}\right]-\mathcal{F}'_{PP}(z_b)\Bigg\{(m_1+m_2)m_3 + \frac{t}{1+t}[-(\alpha_1+\alpha_2)(m_1m_3+m_2m_3-m_1m_2)+\alpha_1p^2+\alpha_2p'^2] -\left(\frac{t}{1+t}\right)^2\left(2-(\alpha_1+\alpha_2)\frac{t}{1+t}\right)[(\alpha_1+\alpha_2)(\alpha_1p^2+\alpha_2p'^2)-\alpha_1\alpha_2q^2]\Bigg\},$$

$$z_b=t\left(\sum_{i=1}^3\alpha_i m_i^2-\alpha_1\alpha_3p^2-\alpha_2\alpha_3p'^2-\alpha_1\alpha_2q^2\right)-\frac{t}{1+t}P_b^2,\quad P_b=\alpha_1p+\alpha_2p'.$$

For the corresponding $c\to s,d$ form factor one has

$$\{\cdots\}^c_{f_+}=-\mathcal{F}_{PP}(z_c)\frac{1}{1+t}\left[1+3\alpha_1\frac{t}{1+t}\right]+\mathcal{F}'_{PP}(z_c)\Bigg\{m_2m_3 + \frac{t}{1+t}[\alpha_1(m_1m_2+m_1m_3-m_2m_3)+\alpha_2q^2]+\left(\frac{t}{1+t}\right)^2[\alpha_1^2p^2-\alpha_2^2q^2)] -\left(\frac{t}{1+t}\right)^3\alpha_1[\alpha_1(\alpha_1+\alpha_2)p^2-\alpha_1\alpha_2p'^2+\alpha_2(\alpha_1+\alpha_2)q^2]\Bigg\},$$

$$z_c = t\left(\sum_{i=1}^{3}\alpha_i m_i^2 - \alpha_1\alpha_3 p^2 - \alpha_2\alpha_3 q^2 - \alpha_1\alpha_2 p'^2\right) - \frac{t}{1+t}P_c^2, \quad P_c = \alpha_1 p + \alpha_2 q.$$

Expressions for the remaining $0^- \to 0^-$ and $0^- \to 1^-$ form factors f_-, A_i and V are given in the Appendix. The masses m_i $(i=1,2,3)$ appearing in the form factor expressions are constituent quark masses with a labeling according to Eqs. (4.12) and (4.13). The values of the constituent quark masses as well as the vertex functions entering the form factor expressions will be specified in Sec. VI.

For the calculation of physical quantities it is more convenient to use helicity amplitudes. They are linearly related to the invariant form factors [22]. For the $0^- \to 0^-$ transitions one has

$$H_0(q^2) = \frac{2m_P P}{\sqrt{q^2}} f_+(q^2), \tag{4.17}$$

$$H_t(q^2) = \frac{1}{\sqrt{q^2}}\{(m_P^2 - m_{P'}^2) f_+(q^2) + q^2 f_-(q^2)\}. \tag{4.18}$$

For the $0^- \to 1^-$ transitions one has

$$H_\pm(q^2) = -(m_P + m_V)A_1(q^2) \mp \frac{2m_P P}{(m_P + m_V)} V(q^2), \tag{4.19}$$

$$H_0(q^2) = \frac{1}{2m_V\sqrt{q^2}}\left\{-(m_P^2 - m_V^2 - q^2)(m_P + m_V) \times A_1(q^2) + \frac{4m_P^2 P^2}{m_P + m_V} A_2(q^2)\right\}, \tag{4.20}$$

$$H_t(q^2) = \frac{m_P P}{m_V\sqrt{q^2}}\left\{-(m_P + m_V)A_1(q^2) + (m_P - m_V) \times A_2(q^2) + \frac{q^2}{m_P + m_V} A_3(q^2)\right\}, \tag{4.21}$$

where

$$P = \frac{\sqrt{\lambda(m_P^2, m_H^2, q^2)}}{2m_P} = \frac{[(q_+^2 - q^2)(q_-^2 - q^2)]^{1/2}}{2m_P}$$

with $q_\pm^2 = (m_P \pm m_H)^2$.

Then the partial helicity rates are defined as

$$\frac{d\Gamma_i}{dq^2} = \frac{G_F^2}{(2\pi)^3}|V_{ff'}|^2 \frac{(q^2 - m_l^2)^2 P}{12 m_P^2 q^2}|H_i(q^2)|^2, \quad i = \pm, 0, t, \tag{4.22}$$

where $V_{ff'}$ is the relevant element of the CKM matrix, and m_l is the mass of charged lepton.

Finally, the total partial rates including lepton mass effects can be written as [22]

$$\frac{d\Gamma^{PP'}}{dq^2} = \left(1 + \frac{m_l^2}{2q^2}\right)\frac{d\Gamma_0^{PP'}}{dq^2} + 3\frac{m_l^2}{2q^2}\frac{d\Gamma_t^{PP'}}{dq^2}, \tag{4.23}$$

$$\frac{d\Gamma^{PV}}{dq^2} = \left(1 + \frac{m_l^2}{2q^2}\right)\left[\frac{d\Gamma_+^{PV}}{dq^2} + \frac{d\Gamma_-^{PV}}{dq^2} + \frac{d\Gamma_0^{PV}}{dq^2}\right] + 3\frac{m_l^2}{2q^2}\frac{d\Gamma_t^{PV}}{dq^2}. \tag{4.24}$$

In the following we shall present numerical results of the total decay widths, polarization ratio and forward-backward asymmetry. The relevant expressions are given by

$$\Gamma = \int_{m_l^2}^{(m_P - m_H)^2} dq^2 \frac{d\Gamma}{dq^2}, \quad \alpha = 2\frac{\Gamma_0}{\Gamma_+ + \Gamma_-} - 1, \quad A_{FB} = \frac{3}{4}\frac{\Gamma_- - \Gamma_+}{\Gamma}. \tag{4.25}$$

V. HEAVY QUARK SPIN SYMMETRY

Our model allows us to evaluate form factors directly from Eq. (4.16) without any approximation. However, it would be interesting to explore whether the heavy quark spin symmetry relations derived in Ref. [4] can be reproduced in our approach. As was shown (see, for instance, [17]) our model exhibits all consequences of the spin-flavor symmetry for the heavy-light systems in the heavy quark limit. For example, the quark-meson coupling and leptonic decay constants behave as

$$g_H \to \sqrt{2m_1}\frac{2\pi}{\sqrt{3\tilde{N}_H}},$$

$$\tilde{N}_H = \int_0^\infty du\, \phi_H^2(u - 2E\sqrt{u})\frac{m_3 + \sqrt{u}}{m_3^2 + u - 2E\sqrt{u}}, \tag{5.1}$$

$$f_H \to \frac{1}{\sqrt{m_1}}\sqrt{\frac{3}{2\pi^2\tilde{N}_H}}\int_0^\infty du[\sqrt{u} - E]\phi_H(u - 2E\sqrt{u}) \times \frac{m_3 + \sqrt{u}/2}{m_3^2 + u - 2E\sqrt{u}}, \tag{5.2}$$

in the heavy quark limit: $p^2 = m_H^2 = (m_1 + E)^2$ when $m_1 \to \infty$. Equations (5.1) and (5.2) make the heavy quark mass dependence of the coupling factors g_H and f_H explicit since

we have factorized the coupling factor contributions into a heavy mass dependent piece and a remaining heavy mass independent piece. Moreover, Eqs. (5.1) and (5.2) show g_H and f_H scale as $m_1^{1/2}$ and $m_1^{-1/2}$, respectively.

As is well known (see Ref. [4]), heavy flavor symmetry cannot be used for hadrons containing two heavy quarks. But one can still derive relations near zero recoil by using heavy quark spin symmetry.

First, we consider the semileptonic decays $B_c \to \overline{B}_s(\overline{B}^0)e^+\nu$ and $B_c \to \overline{B}_s^*(\overline{B}^{*0})e^+\nu$ which correspond to c decay into light s and d quarks, respectively. Since the energy released in such decays is much less than the mass of the b quark, the four-velocity of the B_c meson is almost unaffected. Then the initial and final meson momenta can be written as

$$p = m_{B_c} v, \quad p' = m_B v + r,$$

where r is a small residual momentum $[v \cdot r = -r^2/(2m_B)]$. The heavy quark spin symmetry can be realized in the following way. We split the B-meson masses into the sum of b-quark mass and binding energy:

$$m_{B_c} \equiv m_P = m_1 + E_1, \quad m_B \equiv m_H = m_1 + E_2.$$

Then we go to the heavy quark mass limit $m_b \equiv m_1 \to \infty$ in which the b-quark propagator acquires the form

$$\frac{1}{m_1 - \not p - \not k} \Rightarrow \frac{1 + \not v}{-2(kv + E_1)}. \tag{5.3}$$

The decoupling of the c-quark spin allows us to reliably neglect the k integration because k is small compare to the heavy c-quark mass. One has

$$\frac{1}{m_3 - \not k} \Rightarrow \frac{1}{m_3}. \tag{5.4}$$

As a consequence, the hadronic matrix element describing the weak c-quark decay simplifies:

$$M_c^\mu = \frac{\sqrt{2m_P \cdot 2m_H}}{\sqrt{\tilde N_P \cdot \tilde N_H}} \frac{1}{m_3} \int \frac{d^4k}{4\pi^2 i} \mathcal{F}_{PH}(-k^2) \times \frac{\mathrm{tr}[O^\mu (m_2 + \not k + \not q)\Gamma_H (1 + \not v)\gamma^5]}{[-2kv - 2E_1][m_2^2 - (k+q)^2]}, \tag{5.5}$$

where $q = p - p' = (m_P - m_H)v - r = (E_1 - E_2)v - r \equiv \Delta E v - r$ and m_2 stands for the light quark mass ($m_2 = m_s$ or m_d). One has to emphasize that all above approximations are valid only close to the zero-recoil point $q^2_{\max} = \Delta E^2$. Recalling the transversality of the final vector meson field $p' \cdot \epsilon^* = m_B v + r \cdot \epsilon^* = 0$ and applying the integrations as described in Sec. III, one finds

$$M_c^\mu = \frac{\sqrt{2m_P \cdot 2m_H}}{\sqrt{\tilde N_P \cdot \tilde N_H}} \frac{1}{m_3} \int_0^\infty \frac{dt\, t}{(1+t)^2} \int_0^\infty d\alpha \mathcal{F}_{PH}(z_c) \times \{\cdots\}_{PH},$$

$$\{\cdots\}_{PP} = -\left(m_2 + \frac{\alpha t - \Delta E}{1+t}\right) v^\mu - \frac{1}{1+t} r^\mu,$$

$$i\{\cdots\}_{PV} = -i\varepsilon^{\mu\nu\alpha\beta} \epsilon^{*}{}^{\nu} v^\alpha r^\beta \times \frac{1}{1+t} + \left(m_2 + \frac{\alpha t - \Delta E}{1+t}\right) \epsilon^{*\mu} - \frac{1}{1+t} v^\mu \epsilon^* \cdot r. \tag{5.6}$$

Here, $z_c = [\alpha t^2/(1+t)](\alpha + 2\Delta E) + t(m_2^2 - 2\alpha E_1) - [t/(1+t)]\Delta E^2$. It is readily seen that the amplitudes of c decay in the heavy quark limit are expressed through two independent functions

$$\{\cdots\}_1 = \left(m_2 + \frac{\alpha t - \Delta E}{1+t}\right), \quad \{\cdots\}_2 = \frac{1}{1+t}.$$

To complete the description of the heavy quark limit in the c-decay modes, we give the expressions for the form factors in this limit. One has

$$F(q^2_{\max}) \to \frac{\sqrt{2m_P 2m_H}}{\sqrt{\tilde N_P \tilde N_H}} \int_0^\infty \frac{dt\, t}{(1+t)^2} \int_0^\infty d\alpha \mathcal{F}_{PH}(z_c) \{\cdots\}_F \tag{5.7}$$

where $F = f_\pm, A_i, V$. The form factor specific pieces are given by

$$\{\cdots\}_{f_+} = -\frac{1}{2m_1 m_3}\left(m_2 + \frac{\alpha t}{1+t}\right), \quad \{\cdots\}_{f_-} = \frac{1}{m_3}\frac{1}{1+t},$$

$$\{\cdots\}_{A_1} = -\frac{1}{m_P + m_V}\frac{1}{m_3}\left(m_2 + \frac{\alpha t - \Delta E}{1+t}\right),$$

$$\{\cdots\}_{A_2} = \{\cdots\}_V = \frac{m_P + m_V}{2}\frac{1}{m_1 m_3}\frac{1}{1+t},$$

$$\{\cdots\}_{A_3} = \frac{m_P + m_V}{2}\frac{1}{m_1 m_3}\left[-\frac{3}{1+t} + 4\left(\frac{m_1}{m_3} - 1\right)\frac{t}{1+t}\right].$$

Superficially it appears that the form factors f_+ and A_1 are suppressed by a factor of $1/m_1$. However, they must be kept in the full amplitude to obtain the correct result in Eq. (5.6); for instance, one has

$$f_+(p+p')^\mu + f_-(p-p')^\mu = (2m_1 f_+ + \Delta E f_-)v^\mu + (f_+ - f_-)r^\mu.$$

A similar analysis applies to the $b \to u$ decays $B_c \to (D^0, D^{*0})e^+\nu$. Again the heavy quark symmetry analysis

is only reliable close to zero recoil where the u quark from the $b\to u$ decay has small momentum. One has

$$M_b^\mu=\frac{\sqrt{2m_P\cdot 2m_H}}{\sqrt{\tilde N_P\cdot\tilde N_H}}\,\frac{1}{m_3}\int\frac{d^4k}{4\pi^2 i}\mathcal{F}_{PH}(-k^2)\times\frac{\mathrm{tr}[\gamma^5\Gamma_H(m_2+\not k+\not p')O^\mu(1+\not v)]}{[-2kv-2E_1][m_2^2-(k+p')^2]},\qquad(5.8)$$

where $q=p-p'=(m_1+E_1-m_H)v-r$. The light quark mass m_2 in Eq. (5.8) is the u-quark mass. One finds

$$M_b^\mu=\frac{\sqrt{2m_P 2m_H}}{\sqrt{\tilde N_P\tilde N_H}}\,\frac{1}{m_3}\int_0^\infty\frac{dt\,t}{(1+t)^2}\int_0^\infty d\alpha\mathcal{F}_{PH}(z_b)\{\cdots\}_{PH}\qquad(5.9)$$

with

$$\{\cdots\}_{PP}=\left(m_2+\frac{m_H-\alpha t}{1+t}\right)v^\mu+\frac{1}{1+t}r^\mu,$$

$$i\{\cdots\}_{PV}=-i\varepsilon^{\mu\nu\alpha\beta}\epsilon^{*\nu}v^\alpha r^\beta\left(m_2+\frac{m_H-\alpha t}{1+t}\right)-\frac{1}{1+t}v^\mu\epsilon^*\cdot r.$$

Here, $z_b=[\alpha t^2/(1+t)]\ (\alpha+2m_H)+t\ (m_2^2-2\alpha E_1)-[t/(1+t)]m_H^2$. Again, the amplitudes for the $b\to u$ decays are expressed through two independent functions. The expressions for the form factors in the heavy quark limit close to zero recoil read

$$F(q^2_{\max})\to\frac{\sqrt{2m_P 2m_H}}{\sqrt{\tilde N_P\tilde N_H}}\int_0^\infty\frac{dt\,t}{(1+t)^2}\int_0^\infty d\alpha\mathcal{F}_{PH}(z_c)\{\cdots\}_F,\qquad(5.10)$$

where $F=f_\pm, A_i, V$ and where

$$\{\cdots\}_{f_+}=-\{\cdots\}_{f_-}=\frac{1}{2m_3}\,\frac{1}{1+t},$$

TABLE I. Leptonic decay constants f_H (MeV) used in the least-squares fit.

Meson	This model	Other	Ref.
π^+	131	$130.7\pm0.1\pm0.36$	Expt. [35]
K^+	160	$159.8\pm1.4\pm0.44$	Expt. [35]
D^+	191	191^{+19}_{-28}	Lattice [23,24]
		$192\pm11^{+16+15}_{-8-0}$	Lattice [25]
		$194^{+14}_{-10}\pm10$	Lattice [26]
D_s^+	206	206^{+18}_{-28}	Lattice [23,24]
		$210\pm9^{+25+17}_{-9-1}$	Lattice [25]
		$213^{+14}_{-11}\pm11$	Lattice [26]
B^+	172	172^{+27}_{-31}	Lattice [23,24]
		$157\pm11^{+25+23}_{-9-0}$	Lattice [25]
		$164^{+14}_{-11}\pm8$	Lattice [26]
B_s^+	196	$171\pm10^{+34+27}_{-9-2}$	Lattice [25]
		$185^{+13}_{-8}\pm9$	Lattice [26]
B_c		479	Logarithmic potential [27]
		500	Buchmüller-Tye potential [27]
		512	Power-law potential [27]
		687	Cornell potential [27]
		480	Potential model [6]
		432	QCD-inspired QM [28]
		400 ± 20	QCD spectral SR [29]
		300	QCD SR [30]
		360 ± 60	QCD SR [31]
		300 ± 65	QCD SR [32]
		385 ± 25	QCD SR [33]
		420(13)	Lattice NRQCD [34]
B_c	360	360	Our average of QCD SR
J/ψ	404	405 ± 17	Expt. [35]
Υ	711	710 ± 37	Expt. [35]

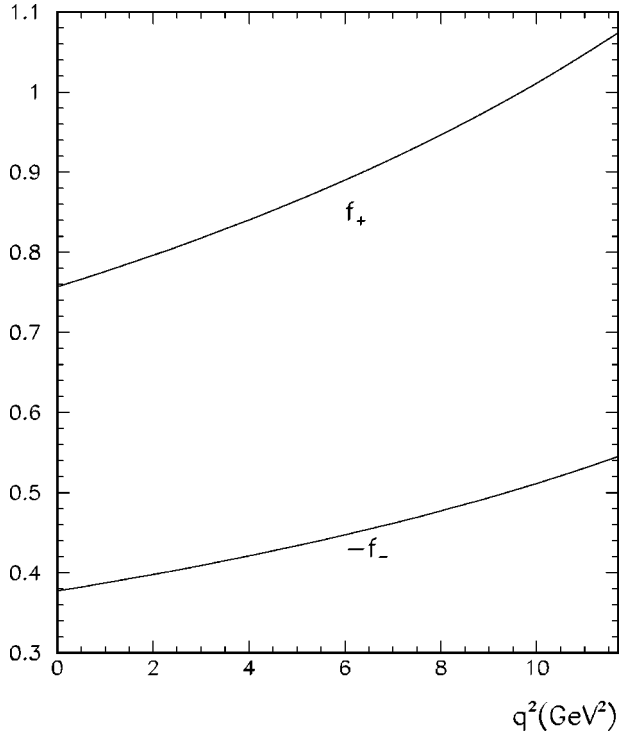

FIG. 9. q^2 dependence of the $B_c \to \eta_c$ form factors. Note that we plot the negative of the $f_-(q^2)$ form factor.

$$\{\cdots\}_{A_1} = \frac{1}{m_P + m_V}\frac{1}{m_3}\left(m_2 + \frac{m_H - \alpha t}{1+t}\right),$$

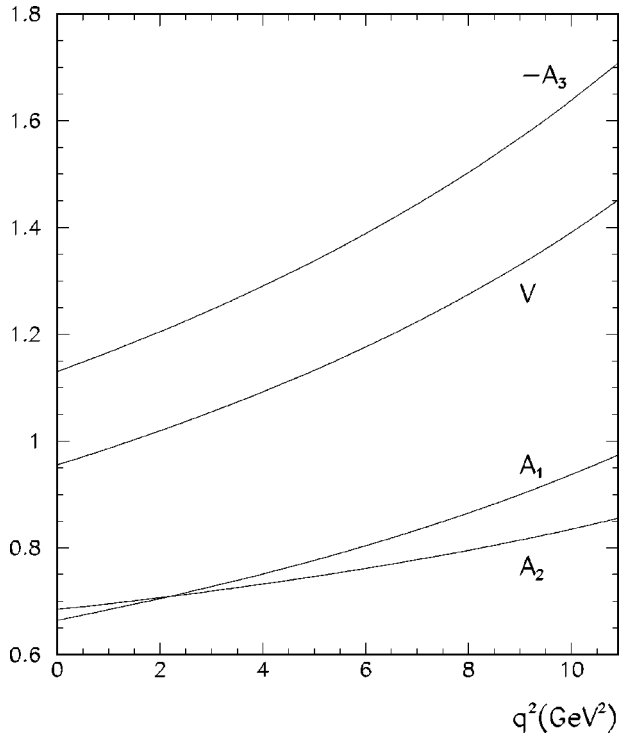

FIG. 10. q^2 dependence of the $B_c \to J/\psi$ form factors. Note that we plot the negative of the $A_3(q^2)$ form factor.

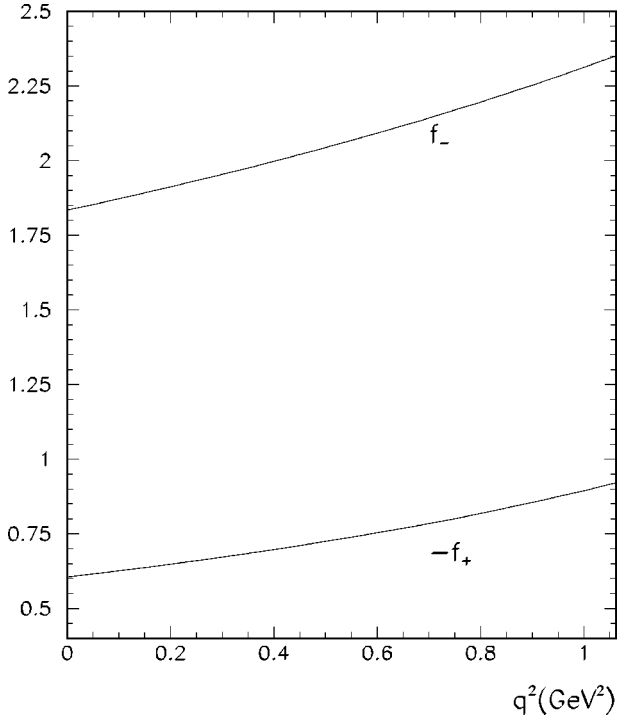

FIG. 11. q^2 dependence of the $B_c \to B_s$ form factors. Note that we plot the negative of the $f_+(q^2)$ form factor.

$$\{\cdots\}_{A_2} = -\{\cdots\}_{A_3} = \{\cdots\}_V = \frac{m_P + m_V}{2}\frac{1}{m_1 m_3}\frac{1}{1+t}.$$

Note that one needs to keep the next-to-leading term in the sum $(f_+ + f_-)$ to obtain the above amplitudes.

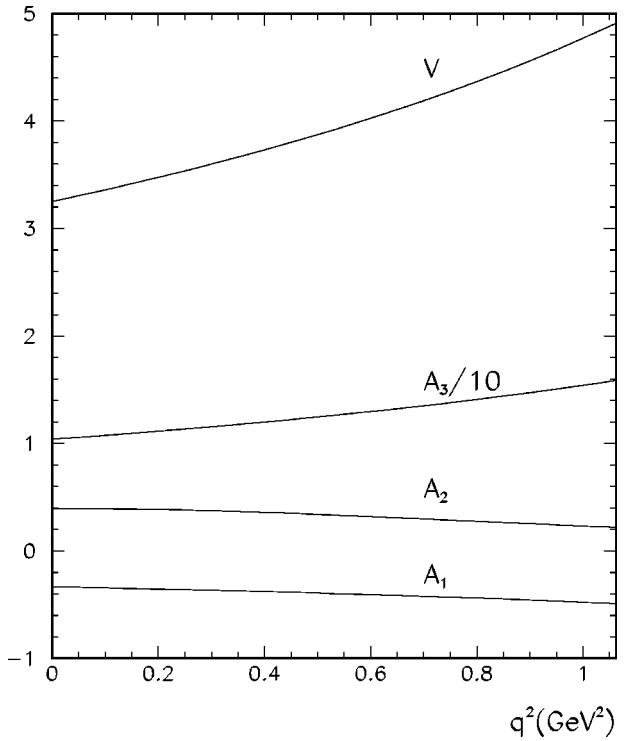

FIG. 12. q^2 dependence of the $B_c \to B_s^*$ form factors.

TABLE II. Predictions for the form factors at $q^2=0$ and $q^2=q^2_{\max}$ for $B_c\to P$ decays.

P	$f_+(0)$	$f_+(q^2_{\max})$	$f_-(0)$	$f_-(q^2_{\max})$
η_c	0.76	1.07	−0.38	−0.55
D	0.69	2.20	−0.64	−2.14
B	−0.58	−0.96	2.14	2.98
B_s	−0.61	−0.92	1.83	2.35

The hadronic matrix elements of the $b\to c$ decays $B_c\to(\eta_c, J/\psi)e^+\nu$ simplify significantly in the heavy quark limit. In this case both b and c propagators may be replaced by their heavy quark limit forms in Eq. (5.3) with the same velocity v. Again, the results will be valid only near zero recoil. One has

$$M^\mu_{cc}=\frac{\sqrt{2m_P 2m_H}}{\sqrt{\tilde N_P \tilde N_H}}\frac{1}{m_3}\int\frac{d^4k}{4\pi^2 i}\mathcal{F}_{PH}(-k^2)\times\frac{\mathrm{tr}[\gamma^5\Gamma_H(1+\not v)O^\mu(1+\not v)]}{[-2kv-2E_1][-2kv-2E_2]} \tag{5.11}$$

where $p=(m_1+E_1)v$, $p'=(m_3+E_2)v+r$. One finds

$$M^\mu_{cc}=\frac{\sqrt{2m_P 2m_H}}{\sqrt{\tilde N_P \tilde N_H}}\frac{1}{2m_3}\int_0^\infty du\int_0^1 d\alpha\times\mathcal{F}_{PH}(u-2\sqrt{u}(\alpha E_1+(1-\alpha)E_2))\{\cdots\}_{PH}, \tag{5.12}$$

$$\{\cdots\}_{PP}=+2v^\mu,\quad i\{\cdots\}_{PV}=-2\epsilon^{*\mu}.$$

The form factors are written down

$$F(q^2_{\max})\to\frac{\sqrt{2m_P 2m_H}}{\sqrt{\tilde N_P \tilde N_H}}\int_0^\infty du\int_0^1 d\alpha\times\mathcal{F}_{PH}(u-2\sqrt{u}(\alpha E_1+(1-\alpha)E_2))\{\cdots\}_F \tag{5.13}$$

where $F=f_\pm, A_i, V$. We have

TABLE III. Predictions for the form factors at $q^2=0$ for $B_c\to V$ decays.

V	$A_1(0)$	$A_2(0)$	$A_3(0)$	$V(0)$
J/ψ	0.68	0.66	−1.13	0.96
D^*	0.56	0.64	−1.17	0.98
B^*	−0.27	0.60	10.8	3.27
B_s^*	−0.33	0.40	10.4	3.25

TABLE IV. Predictions for the form factors at $q^2=q^2_{\max}$ for $B_c\to V$ decays.

V	$A_1(q^2_{\max})$	$A_2(q^2_{\max})$	$A_3(q^2_{\max})$	$V(q^2_{\max})$
J/ψ	0.86	0.97	−1.71	1.45
D^*	0.85	1.76	−3.69	3.26
B^*	−0.42	0.49	18.0	5.32
B_s^*	−0.49	0.21	15.9	4.91

$$\{\cdots\}_{f_+}=\frac{m_1+m_3}{4m_1m_3^2},\quad \{\cdots\}_{f_-}=-\frac{m_1-m_3}{4m_1m_3^2},$$

$$\{\cdots\}_{A_1}=\frac{1}{m_P+m_V}\frac{1}{m_3},$$

$$\{\cdots\}_{A_2}=-\{\cdots\}_{A_3}=\{\cdots\}_V=\frac{m_P+m_V}{4m_1m_3^2}.$$

Thus, our quark loop calculations reproduce the heavy quark limit relations between form factors obtained in [4] near zero recoil. Moreover, we give explicit expressions for the reduced set of form factors in this limit.

VI. RESULTS AND DISCUSSION

Before presenting our numerical results we need to specify our values for the constituent quark masses and shapes of the vertex functions. As concerns the vertex functions, we found a good description of various physical quantities [17] adopting a Gaussian form for them. Here we apply the same procedure using $\phi_H(k^2)=\exp\{-k^2/\Lambda_H^2\}$ in the Euclidean region. The magnitude of Λ_H characterizes the size of the vertex function and is an adjustable parameter in our model. We reiterate that all the analytical results presented in Sec. V are valid for any choice of form factor $\phi_H(k^2)$. For example, we have reproduced the results of [21] where dipole form factor was adopted by using our general formula.

In [17] we have studied various decay modes of the π, K, D, D_s, B and B_s mesons. The Λ parameters and the constituent quark masses were determined by a least-squares fit

TABLE V. Comparison of the form factors at the zero recoil point $q^2=q^2_{\max}$ calculated in the heavy quark limit with exact results.

H	f_+	f_-	A_1	A_2	A_3	V
$\eta_c, J/\psi$	1.07	−0.55	0.86	0.97	−1.71	1.45
$\eta_c, J/\psi$ (HQL)	0.70	−0.35	0.37	0.69	−0.69	0.69
D, D^*	2.20	−2.14	0.85	1.76	−3.69	3.26
D, D^* (HQL)	0.59	−0.59	0.18	1.50	−1.50	1.50
B, B^*	−0.96	2.98	−0.42	0.49	18.0	5.32
B, B^* (HQL)	−0.47	1.67	−0.25	1.91	21.47	1.91

TABLE VI. The numerical values of $m^2_{\rm fit}$ (GeV^2) and δ in the form factor parametrization, Eq. (6.3).

		f_+	f_-	A_1	A_2	A_3	V
$B_c\to\eta_c, J/\psi$	$m^2_{\rm fit}$	$(6.37)^2$	$(6.22)^2$	$(8.20)^2$	$(5.91)^2$	$(5.67)^2$	$(5.65)^2$
	δ	0.087	0.060	1.40	0.052	-0.004	0.0013
$B_c\to B_s, B_s^*$	$m^2_{\rm fit}$	$(1.73)^2$	$(2.21)^2$	$(1.86)^2$	$(3.44)^2$	$(1.73)^2$	$(1.76)^2$
	δ	-0.09	0.07	0.13	-107	-0.09	-0.052

to experimental data and lattice determinations. The obtained values for the charm and bottom quarks [see Eq. (6.1)] allow us to consider the low-lying charmonium (η_c and J/ψ) and bottonium (Υ) states, and also the newly observed B_c meson:

$$\frac{m_u \quad m_s \quad m_c \quad m_b}{0.235\ 0.333\ 1.67\ 5.06}. \tag{6.1}$$

Basically we use either the available experimental values or the values of lattice simulations for the leptonic decay constants to adjust the size parameters Λ_H. The value of f_{B_c} is unknown and theoretical predictions for it lie within the 300–600 MeV range. We choose the value of $f_{B_c}=360$ MeV, being the average QCD sum rule predictions, for fitting Λ_{B_c}. The obtained values of Λ_H are listed in Eq. (6.2) as well as the values of f_H in Table I:

$$\frac{\Lambda_\pi \quad \Lambda_K \quad \Lambda_D \quad \Lambda_{D_s} \quad \Lambda_{J/\psi} \quad \Lambda_B \quad \Lambda_{B_s} \quad \Lambda_{B_c} \quad \Lambda_\Upsilon}{1.16\ 1.82\ 1.87\ 1.95\ 2.12\ 2.16\ 2.27\ 2.43\ 4.425}. \tag{6.2}$$

The values of Λ_H are such that $\Lambda_{m_i}<\Lambda_{m_j}$ if $m_i<m_j$. This corresponds to the ordering law for sizes of bound heavy-light states.

The situation with the determination of Λ_{η_c} is quite unusual. Naively one expects that Λ_{η_c} should be the same as $\Lambda_{J/\psi}$. However, in this case the value of the $\eta_c\to\gamma\gamma$ decay width comes out to be 2.5 less than the experimental average. The experimental average can be reached only for a relatively large value of $\Lambda_{\eta_c}=4.51$ GeV. Note that the values of the other observables ($J/\psi\to\eta_c\gamma$ and $B_c\to\eta_c l\nu$ decay rates) are not so sensitive to the choice of Λ_{η_c}:

$$\mathrm{Br}(\eta_c\to\gamma\gamma)=0.031(0.012)\,\%,$$

$$\mathrm{expt}=(0.031\pm0.012)\,\%,$$

$$\mathrm{Br}(J/\psi\to\eta_c\gamma)=0.90(1.00)\,\%, \quad \mathrm{expt}=(1.3\pm0.4)\,\%,$$

$$\mathrm{Br}(B_c\to\eta_c l\nu)=0.98(1.02)\,\%.$$

The values in parentheses correspond to the case of equal sizes for the charmonium states.

We concentrate our study on the semileptonic decays of the B_c meson. To extend the number of modes, we consider

TABLE VII. Branching ratios BR(%) for the semileptonic decays $B_c^+\to Hl^+\nu$, calculated with the CDF central value $\tau(B_c)=0.46$ ps [1].

H	This model	[9,10]	[7]	[6]	[11]	[8]	[21]
$\eta_c e\,\nu$	0.98	0.8 ± 0.1	0.78	1.0	0.15(0.5)	0.6	0.52
$\eta_c\tau\,\nu$	0.27						
$J/\psi e\,\nu$	2.30	2.1 ± 0.4	2.11	2.4	1.5(3.3)	1.2	1.47
$J/\psi\tau\,\nu$	0.59						
$D^0 e\,\nu$	0.018		0.003	0.006	0.0003(0.002)		
$D^0\tau\,\nu$	0.0094						
$D^{*0} e\,\nu$	0.034		0.013	0.019	0.008(0.03)		
$D^{*0}\tau\,\nu$	0.019						
$B^0 e\,\nu$	0.15		0.08	0.16	0.06(0.07)		
$B^{*0} e\,\nu$	0.16		0.25	0.23	0.19(0.22)		
$B_s^0 e\,\nu$	2.00	4.0	1.0	1.86	0.8(0.9)	1.0	0.94
$B_s^{*0} e\,\nu$	2.6	5.0	3.52	3.07	2.3(2.5)		1.44

TABLE VIII. The polarization ratio α and forward-backward asymmetry A_{FB}.

H	α	A_{FB}
J/ψ	1.15	-0.21
D^{*0}	0.10	-0.46
B^{*0}	0.94	0.35
B_s^{*0}	1.09	0.29

also the decays into the vector mesons D^*, B^* and B_s^*. We will use the masses and sizes of their pseudoscalar partners for the numerical evaluation of the form factors to avoid the appearance of imaginary parts in the amplitudes. Such an assumption is justified by the small differences of their physical masses.

In Figs. 9–12 we show the calculated q^2 dependence in the full physical regions of the semileptonic form factors of the CKM-enhanced transitions $B_c \to \eta_c$, $B_c \to J/\psi$ and $B_c \to B_s$, $B_c \to B_s^*$. The values of form factors at maximum and zero recoil are listed in Tables II–IV. The comparison of the exact values of form factors at zero recoil and those obtained in the heavy quark limit is given in Table V. Our results indicate that the corrections to the heavy quark limit at the zero recoil point $q^2 = q^2_{\max}$ can be as large as a factor 2 in b-c transitions and a factor of almost 5 in b-u and c-d transitions. This is not so surprising considering the semileptonic decays of the D meson where similar corrections can amount to a factor of two [16].

The form factors can be *approximated* by the form

$$f(q^2) = \frac{f(0)}{1 - q^2/m_{\rm fit}^2 - \delta(q^2/m_{\rm fit}^2)^2} \tag{6.3}$$

with the dimensionless values of $f(0)$ given in Tables II and III. Note that the form factor $f_+(q^2)$ for the $B_c \to \eta_c$ transition rises with q^2 as is appropriate in the time-like region. When plotted against $\omega = p \cdot p'/(m_{\rm in} \cdot m_{\rm out}) = (m_{\rm in}^2 + m_{\rm out}^2 - q^2)/(2\, m_{\rm in} \cdot m_{\rm out})$, they would fall with ω as one is familiar with heavy quark effective theory.

It is interesting that the obtained values of $m_{\rm fit}^2$ for the CKM-enhanced transitions (see Table VI) are very close to the values of the appropriate lower-lying $(\bar{q}q')$ vector mesons ($m_{B_c^*} \approx m_{B_c} = 6.4$ GeV for $b \to c$, $m_{D_s^*} = 2.11$ GeV for $c \to s$.). The parameter δ characterizes the admixture of a q^4 term in the denominator. Its magnitude is relatively small for all form factors of the CKM-enhanced transitions except A_1 for the $B_c \to J/\psi$ transition and A_2 for $B_c \to B_s^*$ which have a rather flat behavior. This means that those form factors can be reliably approximated by a vector dominance form. However, one cannot approximate the form factors for the CKM-suppressed transitions by a pole-like function only.

We use the calculated form factors in Eq. (4.25) to evaluate the branching ratios for various semileptonic B_c decay modes including their τ modes when they are kinematically accessible. We report the calculated values of a wide range of branching ratios in Table VII. The results of other approaches are also given for comparison. The values of branching ratios of the CKM-enhanced modes with an electron in the final state are of order 1–2 %. The values of branching ratios of the CKM-suppressed modes are considerably less. The modes with a τ lepton in the final state are suppressed due to the reduced phase space in these modes. To complete our predictions for the physical observables we give in Table VIII the values of the polarization ratio and forward-backward asymmetry for the prominent decay modes.

ACKNOWLEDGMENTS

We would like to thank F. Buccella for many interesting discussions. M.A.I. gratefully acknowledges the hospitality of the Theory Groups at Mainz and Naples Universities where this work was completed. His visit at Mainz University was supported by the DFG (Germany) and the Heisenberg-Landau fund. J.G.K. acknowledges partial support by the BMBF (Germany) under contract 06MZ865.

APPENDIX

In this appendix we list the remaining form factor expressions appearing in the curly brackets in Eq. (4.16) which have not been listed in the main text.

b decay:

$$\{\cdots\}^b_{f_-} = -\mathcal{F}_{PP}(z_b)\frac{1}{1+t}\left[3(\alpha_1-\alpha_2)\frac{t}{1+t}\right] + \mathcal{F}'_{PP}(z_b)\Bigg\{(m_1-m_2)m_3 + \frac{t}{1+t}[(\alpha_1-\alpha_2)(m_1m_3+m_2m_3-m_1m_2)$$

$$+\alpha_1 p^2 - \alpha_2 p'^2] - (\alpha_1-\alpha_2)[(\alpha_1+\alpha_2)(\alpha_1 p^2 + \alpha_2 p'^2) - \alpha_1\alpha_2 q^2]\left(\frac{t}{1+t}\right)^3\Bigg\},$$

$$\{\cdots\}^b_{A_1}=\frac{2}{m_P+m_V}\Bigg\{\mathcal{F}_{PV}(z_b)\frac{1}{1+t}(m_1+2m_2-m_3)-\mathcal{F}'_{PV}(z_b)\Bigg[m_1m_2m_3+\frac{1}{2}(p^2+p'^2-q^2)m_3$$
$$+\frac{1}{2}\frac{t}{1+t}\{[\alpha_1m_1+(2\alpha_1+\alpha_2)m_2-(3\alpha_1+\alpha_2)m_3]p^2+[(\alpha_1+2\alpha_2)m_1+\alpha_2m_2-(\alpha_1+3\alpha_2)m_3]p'^2$$
$$-[\alpha_1m_1+\alpha_2m_2-(\alpha_1+\alpha_2)m_3]q^2\}-(m_1+m_2-m_3)[(\alpha_1+\alpha_2)(\alpha_1p^2+\alpha_2p'^2)-\alpha_1\alpha_2q^2]\left(\frac{t}{1+t}\right)^2\Bigg]\Bigg\},$$

$$\{\cdots\}^b_{A_2}=(m_P+m_V)[\mathcal{F}'_{PV}(z_b)]\Bigg\{-m_3-\frac{t}{1+t}[\alpha_1m_1+\alpha_2m_2-(3\alpha_1+\alpha_2)m_3]+2(m_1-m_3)\alpha_1(\alpha_1+\alpha_2)\left(\frac{t}{1+t}\right)^2\Bigg\},$$

$$\{\cdots\}^b_{A_3}=(m_P+m_V)[\mathcal{F}'_{PV}(z_b)]\Bigg\{m_3+\frac{t}{1+t}[\alpha_1m_1+\alpha_2m_2+(\alpha_1-\alpha_2)m_3]+2(m_1-m_3)\alpha_1(\alpha_1-\alpha_2)\left(\frac{t}{1+t}\right)^2\Bigg\},$$

$$\{\cdots\}^b_V=(m_P+m_V)[-\mathcal{F}'_{PV}(z_b)]\Bigg\{m_3+\frac{t}{1+t}[\alpha_1(m_1-m_3)+\alpha_2(m_2-m_3)]\Bigg\}.$$

We use the abbreviations

$$P_b=\alpha_1p+\alpha_2p',\quad z_b=t\Bigg(\sum_{i=1}^{3}\alpha_im_i^2-\alpha_1\alpha_3p^2-\alpha_2\alpha_3p'^2-\alpha_1\alpha_2q^2\Bigg)-\frac{t}{1+t}P_b^2.$$

c decay:

$$\{\cdots\}^c_{f_-}=3\,\mathcal{F}_{PP}(z_c)\frac{1}{1+t}\Bigg[1-(\alpha_1+2\alpha_2)\frac{t}{1+t}\Bigg]+\mathcal{F}'_{PP}(z_c)\Bigg\{-2m_1m_3+m_2m_3+\frac{t}{1+t}[(\alpha_1+2\alpha_2)$$
$$\times(m_1m_2+m_1m_3-m_2m_3)-2(\alpha_1+\alpha_2)p^2+2\alpha_2p'^2-\alpha_2q^2]+\left(\frac{t}{1+t}\right)^2$$
$$\times[(3\alpha_1^2+6\alpha_1\alpha_2+2\alpha_2^2)p^2-2\alpha_2(\alpha_1+\alpha_2)p'^2+\alpha_2(2\alpha_1+3\alpha_2)q^2]$$
$$-\left(\frac{t}{1+t}\right)^3(\alpha_1+2\alpha_2)[\alpha_1(\alpha_1+\alpha_2)p^2-\alpha_1\alpha_2p'^2+\alpha_2(\alpha_1+\alpha_2)q^2]\Bigg\},$$

$$\{\cdots\}^c_{A_1}=\frac{2}{m_P+m_V}\Bigg\{\mathcal{F}_{PV}(z_c)\frac{1}{1+t}(m_1-2m_2-m_3)-\mathcal{F}'_{PV}(z_c)\Bigg[-m_1m_2m_3+\frac{1}{2}(p^2+q^2-p'^2)m_3\Bigg]$$
$$+\frac{1}{2}\frac{t}{1+t}\{[\alpha_1m_1-(2\alpha_1+\alpha_2)m_2-(3\alpha_1+\alpha_2)m_3]p^2+[-\alpha_1m_1+\alpha_2m_2+(\alpha_1+\alpha_2)m_3]p'^2$$
$$+[(\alpha_1+2\alpha_2)m_1-\alpha_2m_2-(\alpha_1+3\alpha_2)m_3]q^2\}-\left(\frac{t}{1+t}\right)^2(m_1-m_2-m_3)[\alpha_1(\alpha_1+\alpha_2)p^2$$
$$+\alpha_2(\alpha_1+\alpha_2)q^2-\alpha_1\alpha_2p'^2]\Bigg\},$$

$$\{\cdots\}^c_{A_2}=(m_P+m_V)[-\mathcal{F}'_{PV}(z_c)]\Bigg\{m_3+\frac{t}{1+t}[\alpha_1m_1-\alpha_2m_2-(3\alpha_1+\alpha_2)m_3]$$
$$-2(m_1-m_3)\alpha_1(\alpha_1+\alpha_2)\left(\frac{t}{1+t}\right)^2\Bigg\},$$

$$\{\cdots\}^c_{A_3}=(m_P+m_V)[\mathcal{F}'_{PV}(z_c)]\Bigg\{-3m_3+\frac{t}{1+t}[-(3\alpha_1+4\alpha_2)m_1-\alpha_2 m_2+(5\alpha_1+7\alpha_2)m_3]$$
$$+2(m_1-m_3)(\alpha_1+2\alpha_2)(\alpha_1+\alpha_2)\left(\frac{t}{1+t}\right)^2\Bigg\},$$
$$\{\cdots\}^c_V=(m_P+m_V)[-\mathcal{F}'_{PV}(z_c)]\Bigg\{m_3+\frac{t}{1+t}[\alpha_1(m_1-m_3)+\alpha_2(m_2-m_3)]\Bigg\}.$$

Here we have used the abbreviations

$$P_c=\alpha_1 p+\alpha_2 q,\quad z_c=t\left(\sum_{i=1}^{3}\alpha_i m_i^2-\alpha_1\alpha_3 p^2-\alpha_2\alpha_3 q^2-\alpha_1\alpha_2 p'^2\right)-\frac{t}{1+t}P_c^2.$$

[1] CDF Collaboration, F. Abe *et al.*, Phys. Rev. D **58**, 112004 (1998); Phys. Rev. Lett. **81**, 2432 (1998).
[2] N. Isgur and M.B. Wise, Phys. Lett. B **232**, 113 (1989); *ibid.* **237**, 527 (1990).
[3] B.A. Thacker and G.P. Lepage, Phys. Rev. D **43**, 196 (1991).
[4] E. Jenkins, M. Luke, A.V. Manohar, and M.J. Savage, Nucl. Phys. **B390**, 463 (1993).
[5] S.S. Gershtein *et al.*, hep-ph/9803433; in *Progress in Heavy Quark Physics*, edited by M. Beyer, T. Mannel, and H. Schroder (University of Rostock, Rostock, Germany, 1998), p. 272.
[6] C.-H. Chang and Y.-Q. Chen, Phys. Rev. D **49**, 3399 (1994).
[7] A. Abd El-Hady, J.H. Muñoz, and J.P. Vary, Phys. Rev. D **62**, 014019 (2000).
[8] A.Yu. Anisimov, P.Yu. Kulikov, I.M. Narodetskii, and K.A. Ter-Martirosyan, Phys. At. Nucl. **62**, 1739 (1999).
[9] V.V. Kiselev, A.K. Likhoded, and A.I. Onishchenko, Nucl. Phys. **B259**, 473 (2000).
[10] V.V. Kiselev, A.E. Kovalsky, and A.K. Likhoded, Nucl. Phys. **B585**, 353 (2000).
[11] P. Colangelo and F. De Fazio, Phys. Rev. D **61**, 034012 (2000).
[12] M.A. Ivanov, M.P. Locher, and V.E. Lyubovitskij, Few-Body Syst. **21**, 131 (1996); M.A. Ivanov and V.E. Lyubovitskij, Phys. Lett. B **408**, 435 (1997).
[13] A. Salam, Nuovo Cimento **25**, 224 (1962); S. Weinberg, Phys. Rev. **130**, 776 (1963); K. Hayashi *et al.*, Fortschr. Phys. **15**, 625 (1967).
[14] G.V. Efimov and M.A. Ivanov, Int. J. Mod. Phys. A **4**, 2031 (1989); *The Quark Confinement Model of Hadrons* (IOP, London, 1993).
[15] C.D. Roberts and A.G. Williams, Prog. Part. Nucl. Phys. **33**, 477 (1994).
[16] M.A. Ivanov, Yu.L. Kalinovsky, and C.D. Roberts, Phys. Rev. D **60**, 034018 (1999); M.A. Ivanov, Yu.L. Kalinovsky, P. Maris, and C.D. Roberts, Phys. Lett. B **416**, 29 (1998); Phys. Rev. C **57**, 1991 (1998).
[17] M.A. Ivanov and P. Santorelli, Phys. Lett. B **456**, 248 (1999).
[18] M.A. Ivanov, V.E. Lyubovitskij, J.G. Körner, and P. Kroll, Phys. Rev. D **56**, 348 (1997); M.A. Ivanov, J.G. Körner, V.E. Lyubovitskij, and A.G. Rusetsky, *ibid.* **57**, 5632 (1998); **60**, 094002 (1999); **61**, 114010 (2000).
[19] M.A. Ivanov, J.G. Körner, V.E. Lyubovitskij, and A.G. Rusetsky, Phys. Lett. B **476**, 58 (2000).
[20] A. Deandrea, N. Di Bartolomeo, R. Gatto, G. Nardulli, and A.D. Polosa, Phys. Rev. D **58**, 034004 (1998).
[21] M.A. Nobes and R.M. Woloshyn, J. Phys. C **26**, 1079 (2000).
[22] J.G. Körner and G.A. Schuler, Z. Phys. C **46**, 93 (1990).
[23] J.M. Flynn and C.T. Sachrajda, ''Heavy Quark Physics from Lattice QCD,'' hep-lat/9710057; in *Heavy Flavors II*, edited by A. J. Buras and M. Linder (World Scientific, Singapore, 1997), pp. 402–452.
[24] H. Wittig, Int. J. Mod. Phys. A **12**, 4477 (1997).
[25] C. Bernard *et al.*, Phys. Rev. Lett. **81**, 4812 (1998).
[26] A.X. El-Khadra *et al.*, Phys. Rev. D **58**, 014506 (1998).
[27] E.J. Eichten and C. Quigg, Phys. Rev. D **49**, 5845 (1994).
[28] P. Colangelo and F. De Fazio, Mod. Phys. Lett. A **14**, 2303 (1999).
[29] S. Narison, Phys. Lett. B **210**, 238 (1988).
[30] T.M. Aliev and O. Yilmaz, Nuovo Cimento A **105**, 827 (1992).
[31] P. Colangelo, G. Nardulli, and N. Paver, Z. Phys. C **57**, 43 (1993).
[32] M. Chabab, Phys. Lett. B **325**, 205 (1994).
[33] V.V. Kiselev, Int. J. Mod. Phys. A **11**, 3689 (1996).
[34] B.D. Jones and R.M. Woloshin, Phys. Rev. D **60**, 014502 (1999).
[35] Particle Data Group, C. Caso *et al.*, Eur. Phys. J. C **3**, 1 (1998).